International Journal of Engineering and Advanced Technology (IJEAT)
ISSN: 2249-8958 (Online), Volume-9 Issue-1, October, 2019

Rejection of effect of Non-linearities in a PV Grid Integrated System using VSS-SDLMS Scheme

Satish Choudhury, Byomakesh Dash, Renu Sharma, Bidyadhar Subudhi

Abstract ***The integration of photovoltaic system with existing utility plays a vital role to achieve the sustainable development goals set by renewable energy agencies. The grid integration takes place by following IEEE-519 standards. Number of control strategies have already been implemented to maintain the required standard. A number of issues are encountered during the process of synchronization, such as deterioration of quality of power flow due to sudden changes in loads, switching of power semiconductor devices and variation in solar insolation. To address these aforementioned issues a Variable Step Size Sign Data Least Mean Square (VSS-SDLMS) adaptive algorithm is proposed. The proposed controller makes the reference current adaptive to the adversities. In this paper the effective application of signal processing tool i.e.VSS-SDLMS for the power quality issues is well demonstrated by implementing in a three-phase single stage grid connected Photovoltaic (PV) system. The proposed scheme employs to mitigate the harmonic contents produced due to intentional and non-intentional non-linearities in the overall system to a desired level as per IEEE-519 and also it is maintaining the power factor to unity by controlling the reactive power flow. The transient performance of VSS-SDLMS is compared with the conventional LMS based algorithms. The overall system is modelled using MATLAB/SIMULINK.***

Keywords: SDLMS, LMS, Photovoltaic, Total Harmonic Distortion, Unit Templates

I. INTRODUCTION

The trend of future electricity focuses on renewable sources. The statistical report of World Energy Outlook [1] claims that, by 2060 most of the utility grid will be tied by renewable sources. Looking at the percentage rate of growth of utilization of PV sources, one can claim that, the PV source is the best suitable source to achieve the statistical claim. As per the sustainable development policy use of such sources reduces CO_2 emission to a substantial level. Though the indicator of growth of population in Country like India motivate the researchers to do innovation on renewable sources but it shouts to take care the issues encounter during the process of electrification. The primary criteria in the PV-Grid integration is to maintain the quality of power flow irrespective of disturbances. To ensure the same many researchers proposed many methodologies. One such methodology is synchronous reference frame (SRF) based control algorithm [2]. It is basically estimating the angle of orientation at the grid abnormalities, which helps to mitigate the harmonic contents. It is also noticed that, though it fits to mitigate the harmonic content but its dynamic responses are poor in nature. To address the aforesaid issues relating to dynamic response, LMS [3] algorithm is proposed, which claims to have faster dynamic response than SRF. Use of fixed step size in LMS algorithm, decreases the robustness of the system and it is also notice that the range of step size is minimum. The range of the step size is increased using Normalized LMS(NLMS) [4] algorithm by sacrificing the amplitude of oscillation in steady as well as dynamic states. Like NLMS, Least Mean forth (LMF) [5], VSS-LMS [6], Filtered-x-LMS [7] and many such algorithms are proposed to take care of the amplitude of oscillation and the robustness of the system. Similarly, the filtering techniques like Mixed Kalman Particle Filter (MKPF) [8], EKF [9], UKF [10], CDAF [11] wavelet filter have been used in the power system application to encounter grid abnormalities. In this paper, VSS-SDLMS scheme is proposed to mitigate the required harmonics, maintain the power factor unity and reduces the amplitude of oscillation to zero and also fasten the convergence rate. VSS-SDLMS scheme uses Incremental Conductance (I&C) MPPT control to maintain the DC-link voltage constant irrespective of solar irradiance. From the analysis of MPPT control schemes [12] it is observed that, Like Perturb and Observe MPPT method, I&C is also effective to extract maximum power from the PV setup.

The proposed algorithm estimates the active and reactive components of the load current using weight updating law for generating the reference grid current. Further the reference grid current along with the actual grid currents are used to generated required pulses for the controlled switches of interfacing voltage source converter (VSC) through hysteresis current controller. The self-regulation of step sizes proposed in the control scheme fastens the rate of convergence and also enhances the performances of the overall system by estimating the weights under steady and transient states. The overall behavior of PV- Grid system is analyzed

Revised Manuscript Received on October 30, 2019.
* Correspondence Author
Satish Choudhury*, Department of Electrical Engineering, Siksha 'O' Anusandhan (Deemed to be University), Bhubaneswar, India. Email: satishchoudhury@soa.ac.in
Byomakesh Dash, Department of Electrical Engineering, Siksha 'O' Anusandhan (Deemed to be University), Bhubaneswar, India.
Renu Sharma, Department of Electrical Engineering, Siksha 'O' Anusandhan (Deemed to be University), Bhubaneswar, India.
Bidyadhar Subudhi, School of Electrical Sciences, IIT GOA, India

with respect to different abnormalities.

The comparison of performance of proposed algorithm with other conventional algorithm is made to witness the benefit of using proposed algorithm.

The objective of the papers are as follows:

- The active and reactive components of the load current is estimated using VSS-SDLMS algorithm.
- The active and reactive unit templets of the grid voltage are estimated.
- I&C MPPT technique is used to harness maximum power irrespective of solar insolation.
- Total harmonic distortion is calculated under steady and transient conditions.
- Unit power factor (UPF) is achieved at the utility side by controlling the reactive power.

In this paper VSS-SDLMS based PV-grid synchronizing control scheme is proposed to satisfy aforementioned objectives. In this control scheme a variable step size is proposed which helps to reduce the amplitude of oscillation during steady and dynamic state when the system is subjected to different non-linearities.

The paper is organised as follows. Following the Introduction in Section I, Section II describes the modelling of PV-Grid System where the detail modelling of the overall system along with the calculation of required system parameters are discussed. The proposed control scheme is also explained in Section II. The simulation results are discussed in Section III and the brief conclusion is cited in Section IV.

II. PV-GRID INTEGRATION SYSTEM

The overall system is shown in Fig.1. The mathematical modelling of the overall system is discussed in the following section. The system consists of a 10kW PV Array, where the PV modules are interconnected in series parallel fashion to accommodate required amount of voltages and currents, DC-link Capacitor to interface the PV module with the VSC, I&C MPPT controller, interfacing inductor to eliminate current ripple as well as to protect from high inrush current and shunt filter to reduce the ripple content in the voltage across VSC, and the proposed VSS-SDLMS control scheme along with hysteresis controller is employed to provide controlled switching pulses to the semiconductor switches.

A. System Parameters

The system parameters are calculated as in [13]. To obtain 10kW PV power required number of series (N_s) and parallel (N_p) combination of modules are calculated and given in Appendix-I. Similarly, the dc-link capacitor (C_{dc_link}) required to maintain a constant dc-link voltage (Vdc_link) of 700V and to maintain the ripple content below 2% is also given in Appendix-I. Appendix-I also mentions the value of interfacing inductor which is required to maintain the ripple current below 5% as per IEEE-519 standard[14].

B. I&C MPPT Scheme

The basic element of VSS-SDLMS is I&C based MPPT control scheme. It is used for extracting maximum power from PV array irrespective of atmospheric condition and it is also helping to estimate the dc link reference voltage (V_{dc_ref}) which held constant. The pictorial representation of execution of algorithm is shown in Fig.2. It shows the variation of V_{dc_ref} with reference to change in dP_t/dv_t .From the mathematical analysis of I&C MPPT, it is analyzed that, the maximum power is attained when,

$$\frac{dP_t}{dv_t} = 0 \Rightarrow \frac{i_{pv}}{v_t} + \frac{di_t}{dv_t} = 0 \quad (1)$$

where P_t is the PV power, v_t is the voltage across PV array and i_t is the current through PV array.

An integral regulator (IR) is used along with I&C to minimize the error shown in left hand side of (1). Minimization of error helps to track the maximum power at different irradiance. This method is well adaptive towards quick changing atmospheric condition.

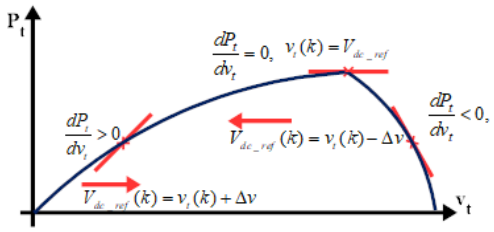

Fig.2. Pt Vs v_t characteristic showing the increment and decrement of V_{dc_ref}.

C. VSS-SDLMS based control scheme

The proposed VSS-SDLMS method uses the estimated V_{dc_ref} from I&C to generate the reference grid current following the process mentioned below. The desired quality of power flow ensuring UPF is only achieved through controlled switching pulses of VSC which is the key element for effective grid integration under adverse condition. The required switching pulses are obtained by passing the current error through a hysteresis band of width 0.01, where the unit of the band width is depending upon the error which is passing through it. In this case it follows the unit of the current i.e. Ampere. The following section depicts the estimation of different control parameters using VSS-SDLMS based control algorithms. The detail control structure is shown in Fig.3.

The following steps are taken into consideration for obtaining reference grid current (i_a^*, i_b^* and i_c^*) through weight updation process using VSS-SDLMS scheme.

Step-1: Calculation of In-phase and quadrature templates:

The in-phase templates (u_{pa}, u_{pb}, u_{pc}) and quadrature component (u_{qa}, u_{qb}, u_{qc}) are calculated using (2) and (3).

$$\begin{bmatrix} u_{pa} \\ u_{pb} \\ u_{pc} \end{bmatrix} = \frac{1}{V_{tp}} \begin{bmatrix} V_a \\ V_b \\ V_c \end{bmatrix} = \frac{1}{V_{tp}} \begin{bmatrix} 2/3 & 1/3 \\ -1/3 & 1/3 \\ -1/3 & -2/3 \end{bmatrix} \begin{bmatrix} V_{ab} \\ V_{bc} \end{bmatrix} \quad (2)$$

$$\begin{bmatrix} u_{qa} \\ u_{qb} \\ u_{qc} \end{bmatrix} = \frac{1}{V_{tp}} \begin{bmatrix} 0 & -1/\sqrt{3} & 1/\sqrt{3} \\ \sqrt{3}/2 & 1/2\sqrt{3} & -1/2\sqrt{3} \\ -\sqrt{3}/2 & 1/2\sqrt{3} & -1/2\sqrt{3} \end{bmatrix} \begin{bmatrix} u_{pa} \\ u_{pb} \\ u_{pc} \end{bmatrix} \quad (3)$$

$$\text{Where } V_{tp} = \sqrt{\frac{2}{3}\left(V_a^2 + V_b^2 + V_c^2\right)} \quad (4)$$

where V_a, V_b and V_c are the phase voltages of 'a', 'b' and 'c' phase respectively and V_{ab} and V_{bc} are the line voltages across phase 'ab' and 'bc' respectively. All the voltages are rated in Volts.

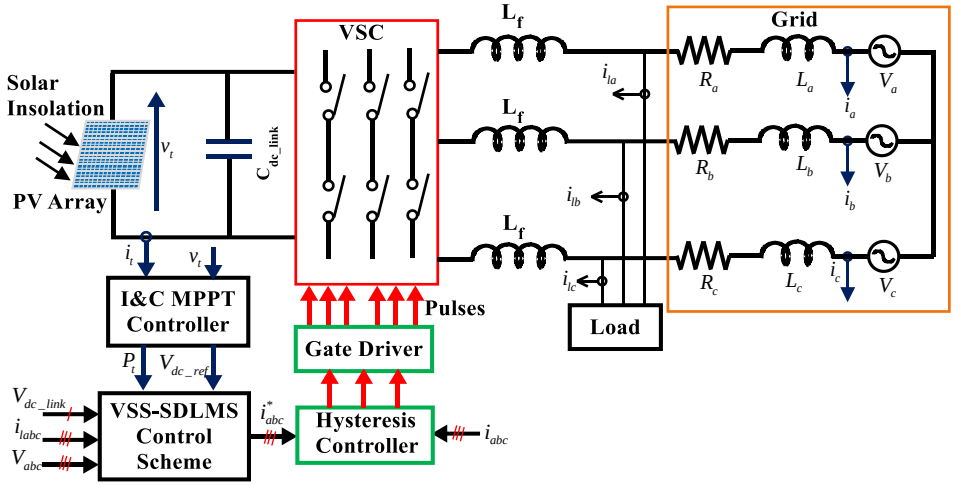

Fig.1. Overall structure of PV-Grid Integration System using VSS-SDLMS Scheme

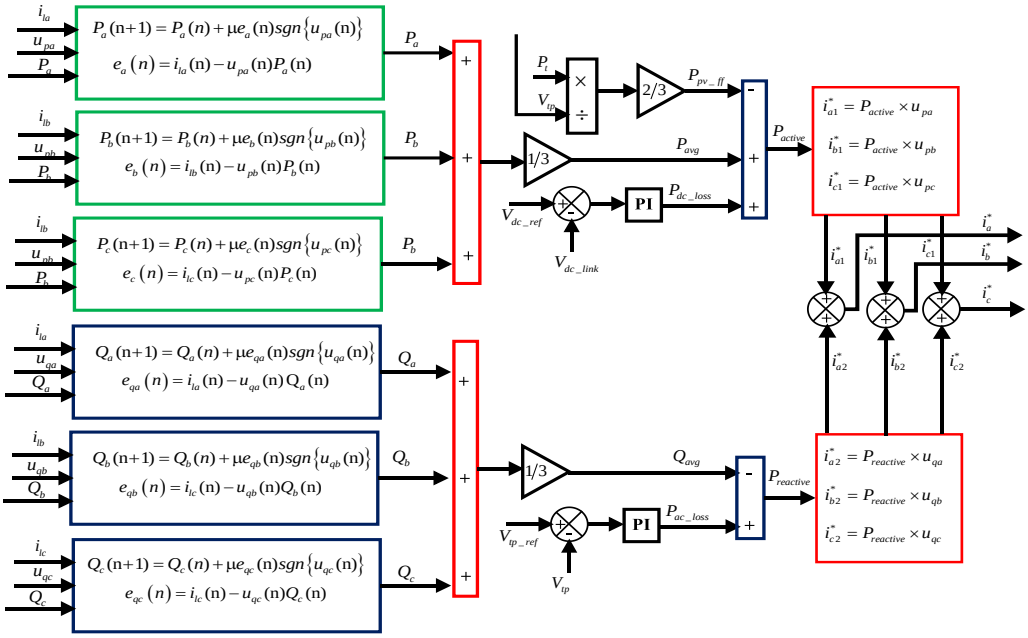

Fig.3. Generation of reference current using VSS-SDLMS control scheme

Step-2: Calculation of DC Power loss:

To maintain the constant V_{dc_link} irrespective of disturbances in grid as well as in PV side it is necessary to calculate DC power loss P_{dc_loss} as in (5).

$$P_{dc\_loss}(k) = P_{dc\_loss}(k-1) + K_c\left(1+\frac{1}{\tau_i s}\right)\left(V_{dc\_ref}(k) - V_{dc\_link}(k)\right) \quad (5)$$

where K_c is the proportional gain and τ_i is the integral time constant of PI controller.

Step-3: Calculation of AC Power loss:

To maintain the ac voltage constant at PCC and to operate the grid-tied system under zero voltage regulation, it is necessary to calculate the AC Power loss P_{dc_loss} as in (6).

$$P_{ac\_loss}(k) = K_{cq}\left(1+\frac{1}{\tau_{iq} s}\right)\left(V_{tp\_ref}(k) - V_{tp}(k)\right) \quad (6)$$

where K_{cq} is the proportional gain and τ_{iq} is the integral time constant of PI controller.

Step-4: Calculation of feed forward component:

The feed-forward components (P_{pv_ff}) used to calculate active weight for the PV system calculated as in (7).

$$P_{pv\_ff} = \frac{2P_t}{3V_{tp}} \quad (7)$$

Step-5: Calculation of Average active weight:
The active weight of 'a' phase load current at each instant 'n' is updated [14] as in (8)

$$P_a(n+1) = P_a(n) + \mu e_a(n) sgn\{u_{pa}(n)\} \quad (8)$$

where $P_a(n)$ is the estimated weight of a-phase load current at 'nth' instant and $e_a(n)$ is the a-phase error. The error is calculated in (9).

$$e_a(n) = i_{la}(n) - u_{pa}(n) P_a(n) \quad (9)$$

At each instant 'n', the kth coefficient can be found by simplifying (8) as in (10)

$$W_{n+1}(k) = W_n(k) + \frac{\mu}{|u_{pa}(n-k)|} e_a(n)\, u_{pa}(n-k) \quad (10)$$

From (10) it is notice that the step size will be different for each co-efficient in the weight vector. Hence the name VSS is attached with SDLMS.
Similarly, the active weights of 'b' and 'c' phase load current $P_b(n)$ and $P_c(n)$ respectively at each instant 'n' is calculated using (8) and (9) replacing the unit templates and error of the respective phases in place of 'a' phase component. For example, 'e_a' will be replaced by 'e_b' for calculation of 'b' phase component and 'e_a' will be replaced by 'e_c' for calculation of 'c' phase components. Similarly, the unit templates u_{pa} will be replaced by u_{pb} and upc for 'b' phase and 'c' phase respectively for the calculation of required weights. The average active weight is calculated using (11).

$$P_{avg} = \frac{P_a(n) + P_b(n) + P_c(n)}{3} \quad (11)$$

Step-6: Calculation of resultant active weight:
The resultant active weight (P_{active}) is calculated in (12)

$$P_{active} = P_{avg} + P_{dc\_loss} - P_{pv\_ff} \quad (12)$$

Step-7: Calculation of Average reactive weights:
The reactive weight of 'a' phase load current at each instant 'n' is updated as in (13)

$$Q_a(n+1) = Q_a(n) + \mu e_{qa}(n) sgn\{u_{qa}(n)\} \quad (13)$$

where $Q_a(n)$ is the estimated weight of a-phase load current at 'nth' instant and $e_{qa}(n)$ is the a-phase error. The error is calculated in (14).

$$e_{qa}(n) = i_{la}(n) - u_{qa}(n) Q_a(n) \quad (14)$$

similarly, the reactive weights of other phase load current i.e. $Q_b(n)$ and $Q_c(n)$ is estimated using (13) and (14)
The average reactive weight is calculated using (15).

$$Q_{avg} = \frac{Q_a(n) + Q_b(n) + Q_c(n)}{3} \quad (15)$$

Step-8: Calculation of resultant reactive weight:
The resultant active weight ($P_{reactive}$) is calculated in (16)

$$P_{reactive} = P_{ac\_loss} - Q_{avg} \quad (16)$$

Step-9: Calculation of reference grid currents:

$$i^*_{a1} = P_{active} \times u_{pa},\ i^*_{b1} = P_{active} \times u_{pb},\ i^*_{c1} = P_{active} \times u_{pc} \quad (17)$$

$$i^*_{a2} = P_{reactive} \times u_{qa},\ i^*_{b2} = P_{reactive} \times u_{qb},\ i^*_{c2} = P_{reactive} \times u_{qc} \quad (18)$$

$$i^*_a = i^*_{a1} + i^*_{a2},\ i^*_b = i^*_{b1} + i^*_{b2},\ i^*_c = i^*_{c1} + i^*_{c2} \quad (19)$$

Step-10: Generation of Switching pulses for VSC:
The error to be compensated using control algorithms stated above is obtained by comparing the calculated reference current from (19) with that of sensed current from utility grid. Then the error is passed through the hysteresis current controller (HCC) operating at width of 0.01. Within the band the actual grid current is tracked to follow the reference grid current through controlled switching patterns of VSC. The schematic diagram is shown in Fig.4.

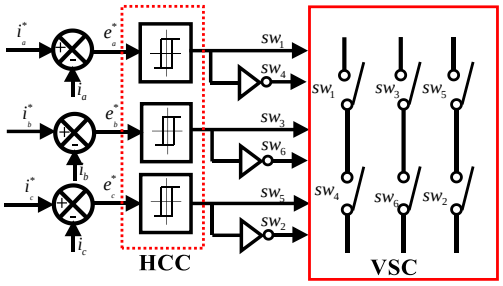

Fig.4. Schematic structure showing generation of switching pulses for VSC

III. RESULTS AND DISCUSSION

The proposed VSS-SDLMS algorithm is simulated using MATLAB/SIMULINK. The complete layout shown in Fig.1 is modelled using MATLAB. A 10kW PV array is implemented for the purpose of simulation choosing suitable numbers of series and parallel modules. I&C MPPT algorithm is used for the purpose of maintaining constant dc link voltage (V_{dc_link}). The steady state and dynamic behavior of the integrated system parameters using proposed VSS-SDLMS algorithm is discussed in the following section.

A. Steady state performance analysis under balanced linear load

The steady state response of the PV-grid integrated system is shown in Fig.5. In this simulation a linear load is taken into consideration for the purpose of analysis. The responses of grid voltage (V_{abc}), grid current(i_{abc}), current through VSC (i_{vsc}), voltage across VSC (V_{vsc}), load current(i_{la}), power extracted from PV array(P_{pv}), voltage across PV array(v_t), current through the PV array(i_t), dc link voltage(V_{dc_link}), active power transmitted to grid (P_g), grid reactive power (Q_g) and active power across load(P_L) are shown.

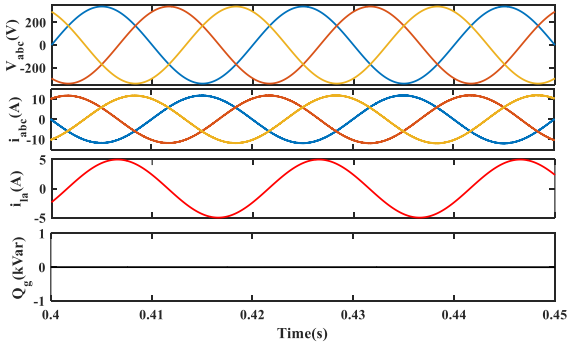

(a)

Retrieval Number: A1794109119/2019©BEIESP
DOI: 10.35940/ijeat.A1794.109119
Journal Website: www.ijeat.org

Published By:
Blue Eyes Intelligence Engineering
& Sciences Publication

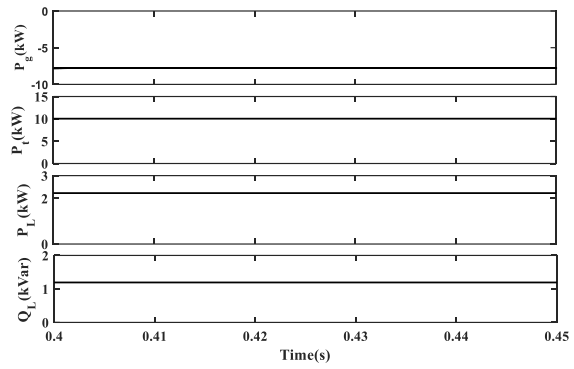

(b)

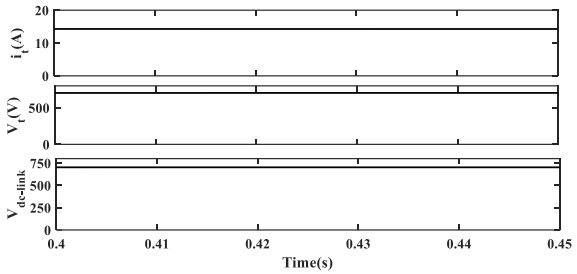

(c)

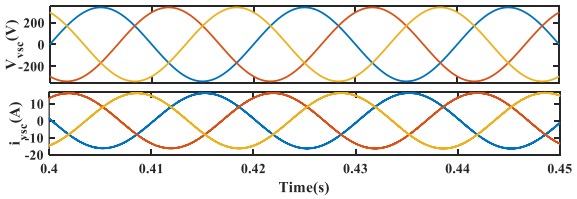

(d)

Fig.5. Simulation results under balanced load. (a) Characteristics of V_{abc}, i_{abc}, i_{la} and Q_g , (b) Characteristics of active powers (P_g,P_t and P_L) and reactive power(Q_L), (c) Characteristics of PV parameters (v_t,i_t and V_{dc_link}) (d) Characteristics of VSC parameters (V_{vsc} and i_{vsc}).

It has been noticed that the objective stated earlier is achieved. Since the reactive power at the grid shown in Fig. 5 (a) is approximately equal to zero, so it shows that the power factor is nearer to unity. DC link voltage is also maintained constant of 700V through MPPT mechanism as witnessed in Fig.5(c). The sharing of power between PV source and utility grid is clearly viewed in Fig.5(b). The negative grid active power indicates the feeding of active power from source to grid. Positive load active power indicates the consumption of active power from PV source. Fig.5(b) shows out of 10kW source power approximately 2.3kW is consumed by the load and remaining 7.7kW is fed to the grid which is negative in nature.

B. Performance analysis under balanced non-linear load

The simulation result of GPIV system with a non-linear load is shown in Fig.6.

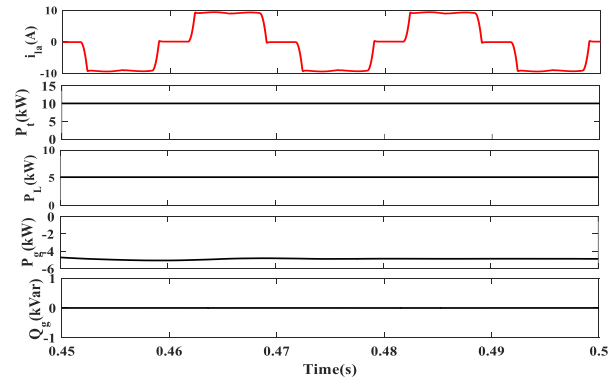

(a)Result analysis of active and reactive Power flow (P_t, P_L, P_g and Q_g)

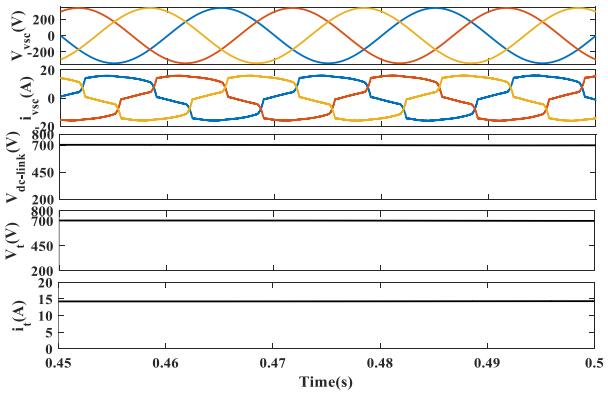

(b) Characteristics of PV and VSC parameters

Fig.6. Simulation results under balanced non-linear load

The load is consisting of a diode bridge rectifier connected with series RL load having R=60Ω and L=100mH. The load voltage is calculated to be 560V using the analysis of three-phase diode bridge rectifier and the power consumed by the load is approximately 5.2kW. The remaining power i.e (P_t-P_L) is fed to the grid. It is also notice that the V_{dc_link} is also maintained constant irrespective of the load switches from linear to non-linear. The changes in load characteristics is witnessing the use of non-linear load.

C. Performance analysis under unbalanced non-linear load

The performance analysis of PV-integrated system is performed under the unbalanced condition where a-phase is disconnected from 0.65s to 0.7s. It has been noticed that irrespective of the disturbances in a-phase the dc link voltage maintained constant at 700V through MPPT technique. It is also observed that when a-phase current is reduced to zero as shown in Fig 7, the power consumed by the load is decreased from 5.2kW to 2.3kW during the period 0.65s to 0.7s. Thus, the power fed to the grid increases to approximately 7 kW excluding losses as shown in Fig.7. The response curve of reactive power is indicating the unit power factor operation during unbalanced condition.

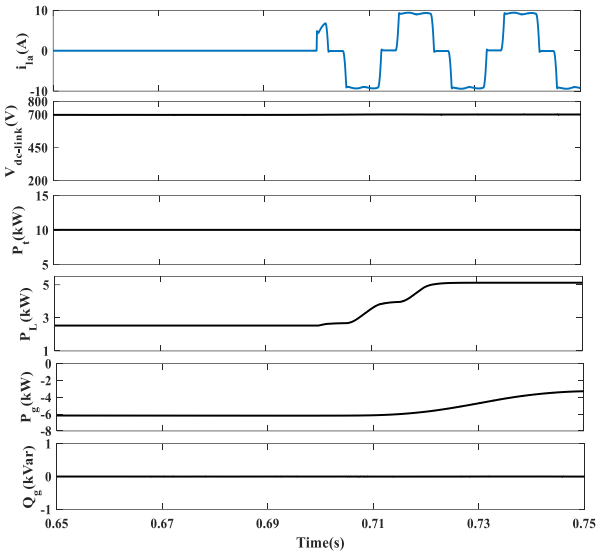

Fig.7. Results of power flow analysis under unbalanced load

D. Performance Analysis under variation of solar irradiance

The performance of the integrated system is analyzed with respect to the variation of solar irradiance (G). From Fig.8, it is observed that when G is very low the grid is supplying active power to the load and at high G the power is fed to the utility grid. From 0.8 to 0.82 the grid active power (P_g) is positive showing supply from grid to load, at approximately 0.86s no power is fed to the grid as total PV power (P_t) is same as the required grid power. From 0.86s onwards PV power is fed to grid which is negative in nature as shown in Fig.8.The power management scheme ensuring UPF operation is analyzed in the given characteristics.

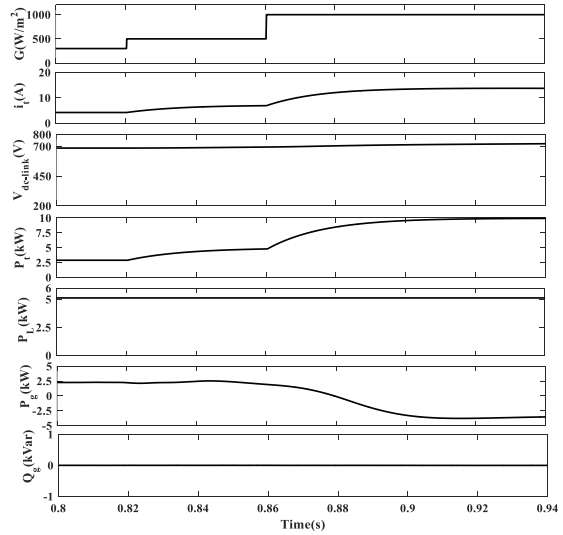

Fig.8. Performance characteristics under variation of solar irradiance

E. Comparative performance analysis of VSS-SDLMS with other conventional methods

To compare the performances of the different algorithms an intentional disturbance in a-phase has been made in simulation during the period 0.5s to 0.7s as shown in Fig.9. Until 0.5s the load sharing by three phases are uniform but from 0.5s to 0.7s loads are unequal. Behavior of the controller using VSS-SDLMS algorithm under steady as well dynamic state has been analyzed in Table 1. To achieve better accuracy during steady and dynamic state and faster convergence rates during dynamic states different step sizes are required. The comparison says that the proposed algorithm is advantageous than other algorithm in achieving both performances.

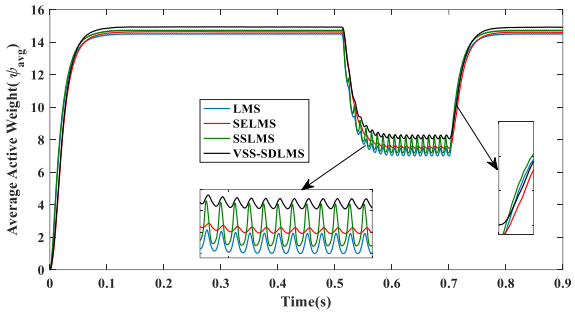

Fig. 9. Comparative Analysis of different LMS based control scheme.

Table -I Comparative result analysis of LMS, SELMS, SSLMS and VSS-SDLMS

Control Algorithm	Steady State Error	Dynamic State Analysis	
		Amplitude of Oscillation	Convergence Rate
LMS	less	medium	fast
SELMS	medium	less	slow
SSLMS	medium	medium	medium
VSS-SDLMS	less	less	fast

IV. CONCLUSION

In this paper, A 10kW PV-grid integrated single stage system supplying power to the non-linear and linear load has been taken into consideration for performance analysis of the control algorithm for different cases. comparative analysis of LMS, SELMS, VSS-SDLMS and SSLMS is made to derive the benefit of VSS-SDLMS. It is also found that the proposed scheme is more suitable to reject the effect of non-linearities as discussed in the results section. Most of the cases it is working with MPPT scheme to maintain the dc link voltage constant and operates at UPF.

APPENDIX

PV voltage =700V, PV power =10kW, Total number of PV modules in series = 24, total number of PV modules in parallel=2, Dc link capacitor =1624μF, Dc link voltage =700V, Interfacing inductor(L_F) = 5.8mH, Line voltage at grid=415V(rms), sampling time (T_s=10^{-6}s. Non-linear Load containing Load resistance(R)=40Ω and Load inductance (L)=100mH.

REFERENCES

1. G. Bridge, S. Barr, S. Bouzarovski, E.Brown, H. Bulkeley, G. Walker, Energy and Society: A Critical Perspective, Routledge, 2018.
2. K.B. Mohanty, S. Choudhury and M.Singh, "Vector Control Realization of DFIG Under Grid Abnormalities using Real Time Digital Simulator", International Journal of Power Electronics and Drive Systems, Vol-7(4), Dec 2016.

3. A. Pradhan, A. Routray, A. Basak, "Power system frequency estimation using least mean square technique", IEEE transactions on power delivery,20 (3) (2005) 1812-1816.
4. S.Pradhan, I. Hussain and B. K. Panigrahi, 'Performance improvement of grid integrated solar PV system using DNLMS control algorithm,' 2016 7th India International Conference on Power Electronics (IICPE), Patiala, 2016, pp. 1-5.
5. N. Beniwal, I. Hussain and B. Singh, 'Hybrid VSS–LMS–LMF based adaptive control of SPV-DSTATCOM system under distorted grid conditions,' in IET Renewable Power Generation, vol. 12, no. 3, pp. 311-322, 26 2 2018.
6. P. Garanayak and G. Panda, 'Fast and accurate measurement of harmonic parameters employing hybrid adaptive linear neural network and filtered-x least mean square algorithm,' in IET Generation, Transmission & Distribution, vol. 10, no. 2, pp. 421-436, 4-2-2016.
7. P. Song, H. Zhao, "Filtered-x least mean square/fourth (fxlms/f) algorithm for active noise control", Mechanical Systems and Signal Processing 120(2019) P.69-82.
8. K. Emami, T. Fernando, H. H. Iu, H. Trinh and K. P. Wong, 'Particle Filter Approach to Dynamic State Estimation of Generators in Power Systems,' in IEEE Transactions on Power Systems, vol. 30, no. 5, pp. 2665-2675, Sept. 2015.
9. E. Ghahremani and I. Kamwa, 'Dynamic State Estimation in Power System by Applying the Extended Kalman Filter With Unknown Inputs to Phasor Measurements,' in IEEE Transactions on Power Systems, vol. 26, no. 4, pp. 2556-2566, Nov. 2011.
10. J. Zhao and L. Mili, 'A Robust Generalized-Maximum Likelihood Unscented Kalman Filter for Power System Dynamic State Estimation,' in IEEE Journal of Selected Topics in Signal Processing, vol. 12, no. 4, pp. 578-592, Aug. 2018.
11. X. Quan, X. Dou, Z. Wu, M. Hu and F. Chen, 'A Concise Discrete Adaptive Filter for Frequency Estimation Under Distorted Three-Phase Voltage,' in IEEE Transactions on Power Electronics, vol. 32, no. 12, pp. 9400-9412, Dec. 2017.
12. A. Rout, S. Samantara, S. Choudhury, et al., 'Modelling and simulation of hybrid MPPT based standalone PV system with upgraded multilevel inverter', Proc. 2014 Annu. IEEE India Conf. (INDICON' 14), pp. 1-6.
13. Al-Haddad, K Chandra, B. Singh, 'Power Quality_ Problems and Mitigation Techniques' -Wiley, 2015, pp.96-137.
14. IEEE recommended practice and requirements for harmonic control in electrical power system, 519-1992.